Available online at www.sciencedirect.com

SciVerse ScienceDirect

Physics Procedia 32 (2012) 165 – 172

Physics Procedia

Conference Title

Deriving Effective Energy Loss Function for Silver from XPS Spectrum

T. Tang[a], Z.M. Zhang[b*], Z.J. Ding[a] and H. Yoshikawa[c]

[a]Hefei National Laboratory for Physical Sciences at Microscale and Department of Physics, University of Science and Technology of China, Hefei, 230026, Anhui, P.R. China

[b]Centre of Physical Experiments, University of Science and Technology of China, Hefei, 230026, Anhui, P.R. China

[c]NIMS Beamline Station at SPring-8, National Institute for Materials Science (NIMS), 1-1-1 Kouto, Sayo-cho, Hyogo 679-5148, Japan

Abstract

XPS spectra of silver excited by synchrotron irradiation with energy same as Al K_α X-ray has been measured. After filtering spectrum noise, the inelastic background starting from the lower binding energy of photoelectrons is removed by an iteration procedure. The energy loss spectrum for a single sub-shell photoelectron is then extracted from the Ag 3*p* XPS spectrum. Based on this single sub-shell photoelectron energy loss spectrum the effective energy loss function (EELF) is obtained by the extended Landau approach. Monte Carlo simulation with the derived EELF can reproduce well the experimental XPS spectrum.

Keywords: XPS; sub-shell photoelectron; effective energy loss function; extended Landau approach; Monte Carlo simulation

* Corresponding author. Tel.: +86 551 360 76 71; fax: +86 551 360 76 71.
E-mail address: zzm@ustc.edu.cn.

 doi:10.1016/j.phpro.2012.03.536

1. Introduction

X-ray photoelectron spectroscopy (XPS) and reflection electron energy-loss spectrum (REELS) are now widely used in the investigation of solid surfaces for providing the information of elemental composition as well as electronic states in the surface region of materials. As the detected electron signals travel some distances in this region before their emission from the surface, they can carry certain information of inelastic interaction with the media. Therefore, those emitted electrons with energy loss in inelastic scattering events contribute to the spectrum feature at lower energy side of no-loss peak. If such an energy loss spectrum for a single no-loss peak is obtained, one can derive the effective energy loss function (EELF) [1-3] of the material from the spectrum feature.

The method to calculate EELF from reflection electron energy loss spectroscopy (REELS) spectrum has already been developed [4-10]. The principle of the method relies on the extended Landau approach [11] for deconvolution of the energy loss spectrum due to a single inelastic event from a multiple inelastic scattering background. The EELF which describes the differential inverse inelastic mean free path (DIIMFP) for this particular experimental condition can then be deduced from this single event energy loss spectrum. A Monte Carlo simulation method [12-14] has been utilized to verify that the derived EELF can indeed reproduce theoretically the experimental REELS spectrum [9-10], while the usual Monte Carlo simulation adopting the optical energy loss function [15] for describing simply the bulk excitation cannot do so for low energy electrons when the surface excitation is no longer negligible.

However, the similar calculation for deriving EELF from a XPS spectrum has not yet been reported. This is because the complexity involved in the deconvolution procedure for XPS spectrum. Firstly, the signal peak is usually superposed on a continuum background due to inelastic scattered electrons of other peaks of lower binding energies. Secondly, except for *s*-orbit photoelectrons two peaks exist in XPS spectra for other orbit photoelectrons; the interval between two peaks for *p*-orbit is larger than that for *d*-orbit. Therefore, the inelastic background due to two peaks may overlap and one has to separate two energy loss spectra for the double peak. In this paper, the EELF is derived from the XPS spectrum for Ag 3*p* electrons. The present work provides an example of the methods used in the calculation procedure: 1, filtering noise; 2, linear background removal; 3, separating the loss spectrum; 4, deconvolution of loss spectrum.

2. Experimental

The XPS spectra were measured with the DAPHNIA attached to the wide-energy-range X-ray beam line BL15XU at SPring-8 in Japan. The two analyzers are put on a turntable that is mounted in a large ultrahigh vacuum (UHV) chamber (base pressure is 6×10^{-8} Pa) of 1400 mm diameter. The take-off angle of each analyzer can be set independently. The rotation axis of a sample manipulator is coincident with the rotation axis of the two analyzers, and the incident SR axis is in the horizontal plane in which the analyzers move. Each electron energy analyzer can measure emitted electrons with kinetic energies less than 4800 eV. X-rays from SR are monochromatized by an YB66 [400] crystal or a Si [111] crystal. Both the analyzers of DAPHNIA are of the spherical-capacitor type with acceptance angles of $\pm5^{o}$. In the experiment, a silver specimen was used because it has been widely used as a reference sample in surface analysis. The sample surface was cleaned by ion bombardment with 3 kV Ar^{+} until impurities could no longer be observed by XPS. The photon flux of the incident monochromatic beam was measured with an Au mesh by detecting the X-ray induced photoelectron current.

The X-ray energy selected from monochromator is 1486.7 eV which is the same as the energy of Al K_{α} X-rays. The energy resolution is limited by the beamline monochromator and the XPS analyzer, and the combined energy resolution for a spectrum is 0.17 eV. The details are described elsewhere [16].

3. Theoretical Methods

The noise in the spectrum may affect the latter processing work significantly. The first step for the spectrum analysis is the filtering by multi-points smoothing or Wiener filtering or wavelet filtering methods [17].

3.1 Linear background removal

The background should be removed in the following analysis of XPS spectrum. In general, the XPS wide spectrum for an element is contributed from a variety of core shell electrons. The higher energy photoelectrons with lower binding energies provide a large inelastic background for lower energy photoelectron peak in the spectrum. Popular Shirley's [18-21] and Tougaard's [22-25] background removal methods aims mainly at providing the inelastic background by photoelectrons of the concerned peak. But here we are considering the large continuum background due to other peaks of lower binding energies, which behaves more like linear line in the interested energy range of the concerned peak, Ag 3*p*. The equation for background removal is expressed as below:

$$F(E) = g(E) + B(E) \tag{1}$$

$$B(E) = b + kE \tag{2}$$

$$g(E) = f(E) + \alpha \cdot f(E + \Delta E) \tag{3}$$

where $F(E)$ is the noise-filtered experimental spectrum for core shell photoelectrons with two sub-shells (e.g., $3p_{1/2}$ and $3p_{3/2}$), $g(E)$ is the XPS spectrum of double peaks after removing the inelastic scattering background $B(E)$ from higher energy photoelectrons. $f(E)$ is the spectrum for a single sub-shell photoelectron peak, which is what we expect to extract from $F(E)$. ΔE is the energy interval between these two sub-shells, and α is the fixed proportion factor which is one in two for *p*-orbit or two in three for *d*-orbit. k is the slope of the linear line and b is the intensity at the starting point of the line. Fig. 1 shows the result of Ag 3*p* XPS spectrum by removing the linear background due to 3*d* photoelectrons.

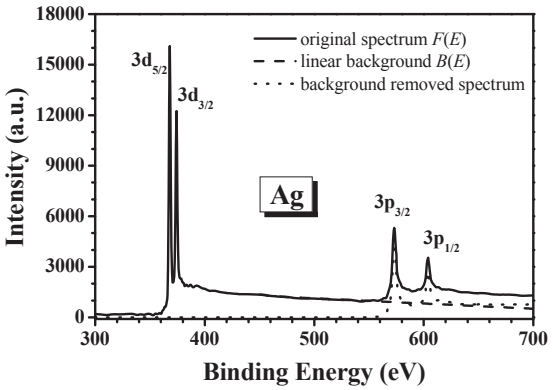

Fig. 1. Removing the linear background for Ag 3*p* peaks.

3.2 Energy loss spectrum for single sub-shell peak

For the same core shell, the photoelectron energy spectrum shape for each sub-shell can be considered as the same because of their little difference in binding energy. Therefore, in Eq. (3) the spectra for two sub-shells are denoted as $f(E)$ and $f(E+\Delta E)$. The spectrum shape of $f(E)$ for a single peak is then extracted from $g(E)$ by an iteration procedure. Figs. 2(a) and 2(b) show the obtained $f(E)$ spectra for Ag 3*p* and 3*d* photoelectrons, respectively. The experimental XPS spectra agree with the addition of the spectra for two sub-shell photoelectrons. It is seen that the XPS spectrum for a single sub-shell, $f(E)$, includes a sharp peak for no-loss signals and a long tail in the lower kinetic energy side due to inelastic scattering of photoelectrons. This corresponds to the energy loss spectrum in REELS.

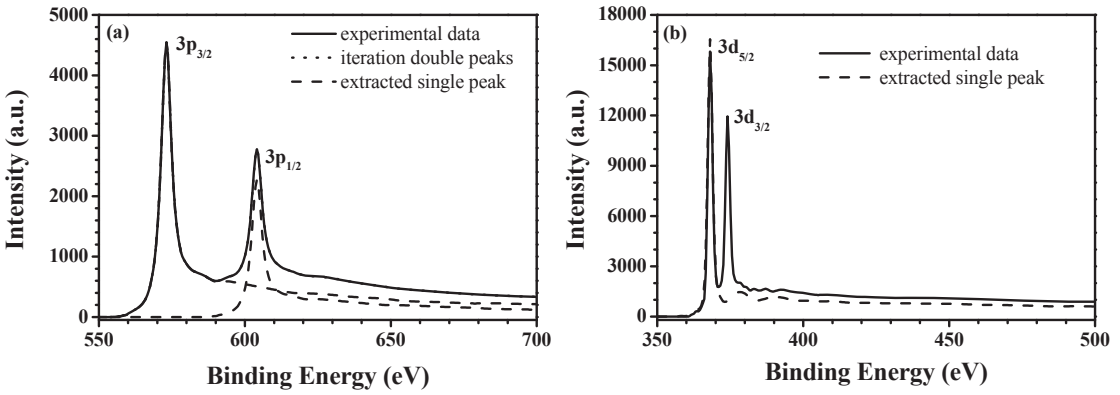

Fig. 2. Extraction of single sub-shell photoelectron spectrum for: (a) Ag $3p_{1/2}$ and $3p_{3/2}$; (b) Ag $3d_{3/2}$ and $3d_{5/2}$.

3.3 Deconvolution of loss spectrum

The spectrum for monochromatic energy has been obtained by deconvoluting of the calculated single sub-shell photoelectron spectrum with the source function for Ag 3*p* in Fig. 2a. The spectrum extracted by deconvoluting contains single scattering contribution as well as multiple scattering components due to bulk and surface excitations. The DIIMFP can then be obtained by the extended Landau approach. Comparing with the REELS case the XPS spectrum exists peak broadening from X-ray source, which may introduce some uncertainty during deconvolution process. Fig. 3 shows the DIIMFP calculated from Ag 3*p* XPS spectrum. The intensity is high at low energy loss region and decays fast at large losses.

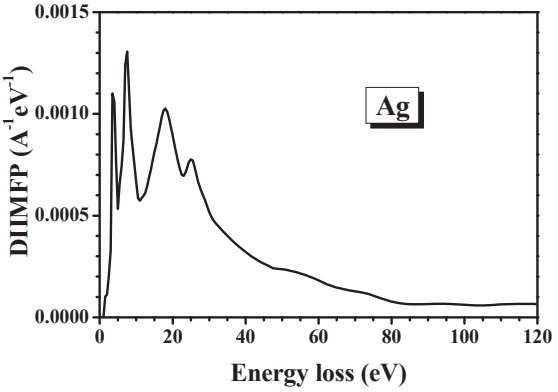

Fig. 3. The differential inverse inelastic mean free path (DIIMFP) derived from Ag 3*p* photoelectron energy loss spectrum.

The calculated EELF from DIIMFP for Ag 3*p* photoelectrons is shown in Fig. 4. The surface energy loss function (SELF) $\mathrm{Im}\{-1/(1+\varepsilon(\omega))\}$ and bulk energy loss function (BELF) $\mathrm{Im}\{-1/\varepsilon(\omega)\}$ [9-10] derived from an optical constant database [26], together with EELF obtained from REELS spectrum for Ag at 1 keV, are compared in Fig. 5. Both EELFs from XPS and REELS spectra include not only bulk excitation but also surface excitation. Each feature in EELF from XPS corresponds well with those in SELF, BELF and EELF from REELS. Particularly, it can be seen that the peak at about 3.5-3.9 eV in present EELF actually comprises of surface excitation peak at 3.7 eV in SELF and bulk excitation at 3.8 eV in BELF. Therefore, the present result is quite reasonable. Fig. 5 shows the Monte Carlo simulation of Ag XPS spectrum for $3p_{3/2}$ single sub-shell by using the derived EELF from Ag 3*p*. The simulation based on EELF from XPS can reproduce the experimental spectrum well.

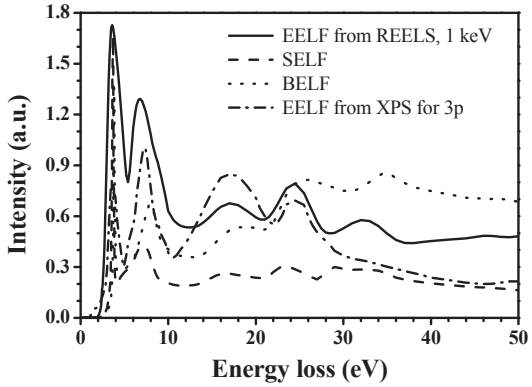

Fig. 4. Comparison on energy loss functions obtained by different methods: the present EELS derived from XPS spectrum for Ag 3p photoelectrons, EELS derived from RELLS spectrum for Ag at 1 keV, surface energy loss function and bulk energy loss functions based on optical constants.

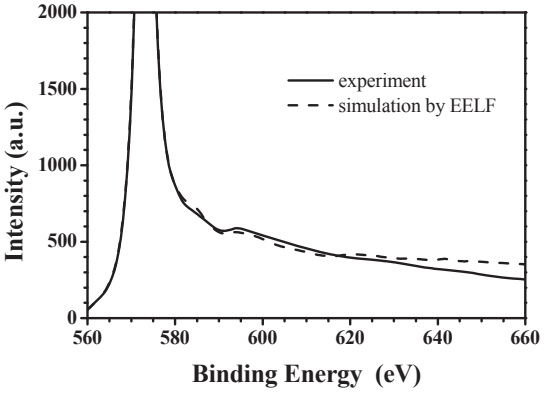

Fig. 5. Comparison of the Ag XPS spectrum for $3p_{3/2}$ single sub-shell between the experiment and Monte Carlo simulation by using the derived EELF for Ag 3*p* photoelectrons.

4. Conclusion

In this work the approach to derive EELF from XPS spectrum of two sub-shells containing large spectrum background is applied to Ag 3*p* photoelectrons. The linear background due to lower binding photoelectrons is firstly removed from the wide Ag XPS spectrum. The energy loss spectrum for single sub-shell photoelectrons is then extracted by iteration. Based on the extended Landau approach the DIIMFP and EELF are obtained from this Ag 3*p* photoelectron energy loss spectrum. The obtained EELF includes not only bulk excitation but also surface excitation. A Monte Carlo simulation has reproduced the experimental XPS spectrum by using this EELF.

Acknowledgements

This work was supported by the National Natural Science Foundation of China (Grant Nos. 11074232 and 10874160), "973" projects (Nos. 2011CB932801 and 2012CB933702) and "111" project. We thank Supercomputing Center of USTC for support to parallel computations.

References

[1] Yoshikawa H, Shimizu R, Ding ZJ. Energy loss function derived by Monte Carlo simulation from the Au 4f XPS spectrum. *Surf Sci* 1992;**261**:403-411.

[2] Yoshikawa H, Tsukamoto T, Shimizu R, Crist V. Monte Carlo analysis of XPS and REELS spectra obtained at different take-off angles. *Surf Interface Anal* 1992;**18**:757-764.

[3] Yoshikawa H, Irokawa Y, Shimizu R. Measurements of reflected electron energy loss spectrometry and X-ray photoelectron spectroscopy spectra for derivations of the energy loss function and source function for Au 4f photoelectrons. *J Vac Sci Technol A* 1995;**13**:1984-9.

[4] Nagatomi T, Ding ZJ, Shimizu R. Derivation of new energy-loss functions as applied to analysis of Si 2p XPS spectra. *Surf Sci* 1996;**359**:163-173.

[5] Nagatomi T, Shimizu R, Ritchie RH. Effective energy-loss functions for oxygen-adsorbed amorphous silicon surfaces. *J Appl Phys* 1999;**85**:4231-7.

[6] Nagatomi T, Shimizu R, Ritchie RH. Energy loss functions for electron energy loss spectroscopy. *Surf Sci* 1999:**419**:158-173.

[7] Nagatomi T, Kawano T, Fujii H, Kusumoto E, Shimizu R. New energy loss functions for 1 keV electrons incident on clean and oxygen-adsorbed Si(111) surfaces. *Surf Sci* 1998;**416**:184-191.

[8] Nagatomi T, Kawano T, Shimizu R. Determination of effective energy loss functions and X-ray photoelectron spectroscopy source functions for Si 2p photoelectrons from clean Si(111) oxygen-adsorbed Si(111) and SiO_2 surfaces. *J Appl Phys* 1998;**83**:8016-8026.

[9] Zhang ZM, Iyasu T, Shimizu R, Goto K, Koshikawa T. Comparison of energy-loss functions from REELS spectra with surface and bulk energy loss functions for Ag. *Surf Interface Anal* 2003;**35**:403-9.

[10] Zhang ZM, Chen T, Ding ZJ, Tang T, Tőkési K. Optical properties of silver thin films derived from REELS. *Surf Interface Anal* 2010;**42**:1303-6.

[11] Landau L. On the energy loss of fast paticles by ionisation. *J Phys (Moscow)* 1944;**8**:201-5.

[12] Ding ZJ, Shimizu R. Inelastic collisions of kV electrons in solids. *Surf Sci* 1989;**222**:313-331.

[13] Ding ZJ. Fundamental studies on the interactions of kV electrons with solids for applications to electron spectroscopies. (PhD thesis, Osaka university); 1990.

[14] Shimizu R, Ding ZJ. Monte Carlo modeling of electron-solid interactions. *Rep Prog Phys* 1992;**55**:487-531.

[15] Penn DR. Electron mean-free-path calculations using a model dielectric function. *Phys Rev B* 1987;**35**:482-6.

[16] Zhang ZM, Ding ZJ, Koshikawa T, Iyasu T, Shimizu R, Yoshikawa H et al.. Angular distribution of X-ray photoelectrons emitted from silver. *Surf Sci* 2005;**592**:18-24.

[17] Kosarev EL, Pantos E. Optimal smoothing of noisy data by fast fourier transform. *J Phys E Sci Instrum* 1983;**16**:537-543.

[18] Shirley DA. High-resolution X-ray photoemission spectrum of the valence bands of gold. *Phys Rev B* 1972;**5**:4709-4714.

[19] Vegh J. The Shirley-equivalent electron inelastic scattering cross-section function. *Surf Sci* 2004;**563**:183-190.

[20] Vegh J. The Shirley background revised. *J Elect Spectrosc* 2006;**151**:159-164.

[21] Castle JE, Salvi AM. Interpretation of the Shirley background in X-ray photoelectron spectroscopy analysis. *J Vac Sci Technol A* 2001;**19**:1170-5.

[22] Tougaard S, Sigmund P. Influence of elastic and inelastic scattering on energy spectra of electrons emitted from solids. *Phys Rev B* 1982;**25**:4452-4466.

[23] Tougaard S. Background removal in X-ray photoelectron spectroscopy: Relative importance of intrinsic and extrinsic processes. *Phys Rev B* 1986;**34**:6779-6783.

[24] Tougaard S. Quantitative analysis of the inelastic background in surface electron spectroscopy. *Surf Interface Anal* 1988;**11**:453-472.

[25] Tougaard S. Practical algorithm for background subtraction. *Surf Sci* 1989;**216**:343-360.

[26] Palik ED. Handbook of Optical Constant of Solid II, New York: Academic Press; 1991.